RESEARCH INTO AERODYNAMICS, FLIGHT DYNAMICS AND STRENGTH OF NEW GENERATION HELICOPTERS AT TsAGI

S.L.Chernyshev and M.A.Golovkin
Central Aerohydrodynamic Institute named after N.Ye.Zhukovsky (TsAGI).
Zhukovsky, Russia

The obtained recently results of TsAGI investigations directed on improvement of aerodynamic, acoustic, flight and ecological characteristics of advanced rotorcraft are presented

SYMBOLS and ACRONIMS

α – angle of attack, degrees;
R – rotor radius;
ω – rotor angle frequency;
C_l – sectional lift coefficient, C_l = [Lift Force]/(05·ϱ V^2/[Frea]);
T – rotor thrust;
b – blade chord;
F – rotor disc area, m^2;
σ – geometric rotor solidity;
C_L – lift coefficient;
C_D – drag coefficient;
C_M – pitching moment coefficient;
C_{M0} – pitching moment coefficient with $C_L = 0$;
C_T – rotor thrust coefficient, $C_T = T/(0.5\varrho(\omega R)^2 F)$;
FM – rotor figure of merit, in hover;
K_{rot} – equivalence rotor aerodynamic quality;

1.INTRODUCTION

In the context of the fact that at present velocity characteristics of classical rotorcraft layout are at present approached extreme capabilities the search of new scientific and technical decisions ensuring creation of advanced high-speed rotorcraft becomes an urgent problem.
The rotorcraft is the complex vehicle both from the view point of aerodynamics and wide spread occurrence of physical processes. For years computational and experimental studies [1] directed to the development of scientific-technical backlog for advanced high-speed rotorcraft were performed in TsAGI. Some main results of these studies are discussed in the given paper.
Computational studies are based both on the known vortex rotor models and on Reynolds averaged equations of Navier-Stokes (RANS/URANS)/ In this case commercial package ANSYS CFX Ver.13.0 [2] was used that was realized on the current computer cluster.
The studied experimental results were obtained in TsAGI T-105 and T-104 wind tunnels.

2.THE MAIN MODERN DIRECTION OF ROTORCRAFT PROGRESS

The modern world trends of rotorcraft progress are associated with

- the increase of flight speed up to 400-500km/h;
- the increase of flight range up to 1000-1500km;
- the decrease of location noise;
- the improvement of comfort (the decrease of noise and vibrations in the cabin);
- the increase of service life;
- the decrease of operating costs;
- the improvement of stability and control characteristics as well as the maneuverability .

In this case certain unfavorable problems grow with the increase of rotorcraft flight speed, in particular:

- rotor lift-to-drag decrease due to flow break-away on retreating blade;
- rotor propulsive capabilities are going down;
- hinge moments increase;
- vibrations increase considerably;
- rotorcraft noise is going up;
- body drag increases.

To decide these problems it is necessary to improve experimental and computational base and to carry out regular object-oriented investigations.

3.AEROFOIL SECTIONS

One of the key elements of aerodynamic design of rotorcraft rotor and tail rotor blades is the blade airfoil section. Several generations of helicopter profiles are developed in TsAGI. New requirements to high-speed rotors determine further development of new helicopter airfoil sections. To increase maximum load-carrying capability of profiles the procedure of local optimization of leading edge shapes for multimode helicopter profiles and new effective method of computational grid building is developed.

The suggested technique is verifies by CFD RANS methods and experimental investigations. High-speed helicopter profiles of TsAGI-5 series were developed with the help of this technique. For the profile of main blade sections it was proposed to increase the maximum lift coefficient C_{lmax} at free stream Mach number $M_\infty \approx 0.4$ as compared to profile-prototype. As a result of performed investigations a considerable increase computational levels of maximum lift coefficient is obtained. The new profile noticeably exceeded profile-prototype by maximum lift coefficient, and by the critical Mach number it remained at the high level similar to TsAGI-4 series profiles.

In the report of Forum-9 it is shown that the new modified profile has excelled the profile-prototype in maximum lift coefficient by the value of $\Delta C_{lmax} = 0.1$ (Fig.1).

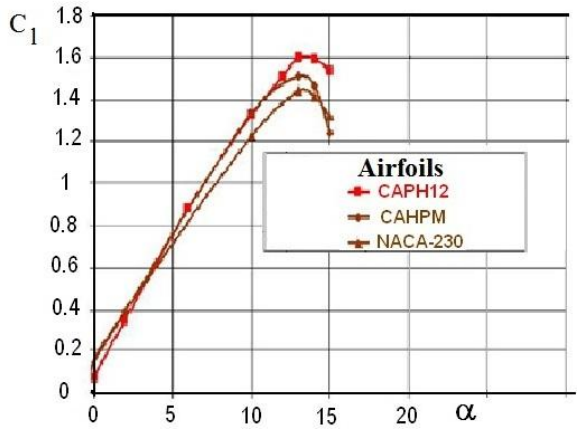

Fig.1. Local optimization of leading edge shape of multimode rotorcraft profiles and its realization.

airfoil

Studies in this direction were continued, and modified variants of profiles for specific blade aerodynamic configurations were used in new designs of advanced high-speed rotors.

3.1. Computation of profile unsteady characteristics

Flow pattern of the NACA 23012 profile oscillating at angle of attack obtained by computation in RNS method [2] is shown in Fig.2.

The moment is presented when the maximum angle of attack is passed and the profile moves in the direction of angle of attack decreasing. At that it is seen that the free vortex is broken away and moves streamwise.

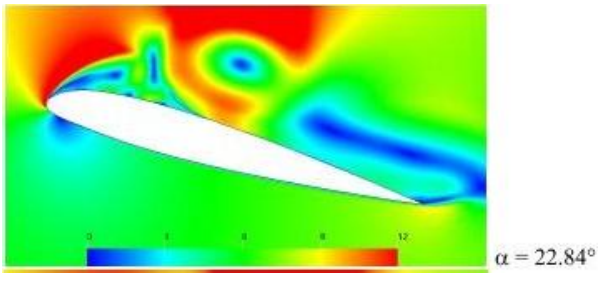

Fig.2. Navier-Stokes computation of airfoil oscillating at angle of attack.

To specify the analysis of experimental results obtained in SVS-2 wind tunnel for oscillating profiles the problem of unsteady flow about the blade section was solved by

RANS methods at flight Mach number (Fig.3). For this purpose the appropriate 3D model of this phenomenon and grid models were built.

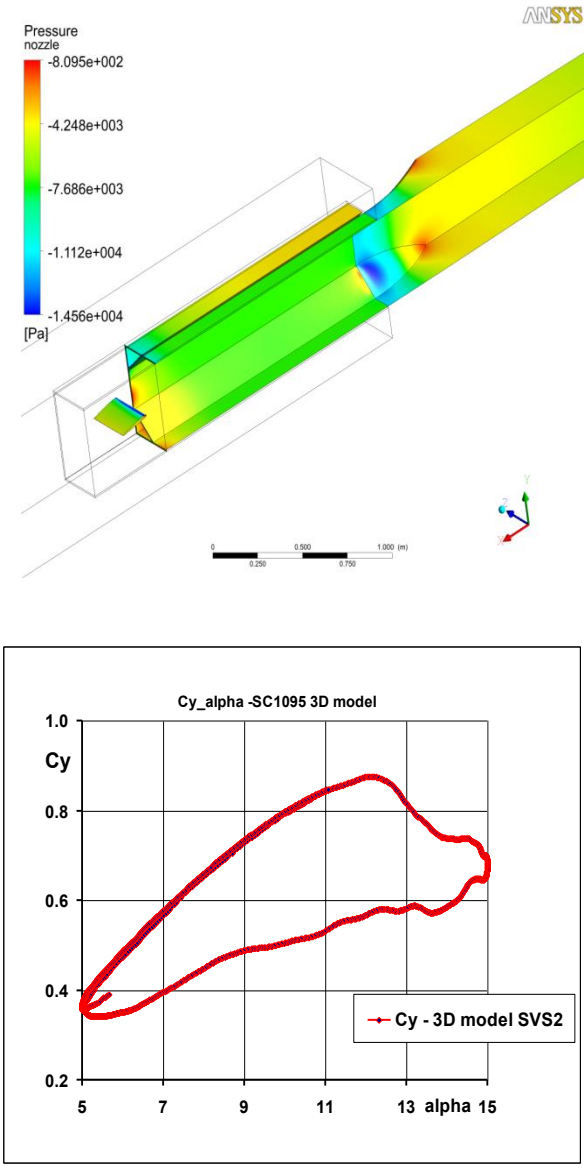

Fig.3. Navier-Stokes computation of blade section oscillating at angle of attack.

3.2.Experimental studies of profile nonstationary characteristics

The regular tests of profiles oscillating at angle of attack were performed in TsAGI for a long time.
With this purpose a special facility DINKR-1 (Fig.4) was developed for subsonic wind tunnel SVS-2, and as well as DINKR-2 – for T-105 wind tunnel.

Bench DINKR-*1* in SVS-*2*

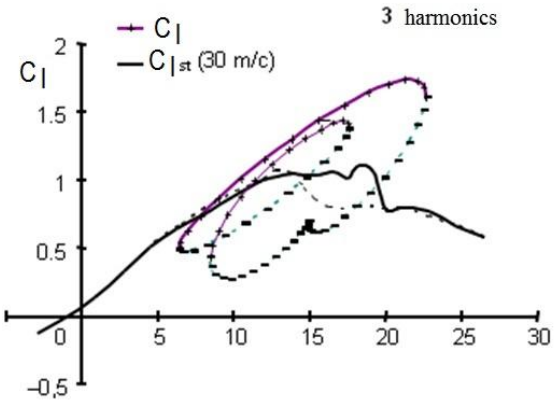

Fig.4. Experimental studies of oscillating profile unsteady characteristics

These facilities permit the testing of profiles oscillating both by the harmonic law and by the sum up to three harmonics (Fig.4).

4.ROTOR AERODYNAMICS

4.1.Development of rotor computational methods based on Reynolds averaged Navier-Stokes equations (RANS/URANS)

Computations of different rotors are performed based on the license version ANSYS CFX 13.0. To verify the used numerical computational method its results were compared with experimental data [3].
These data were obtained while studying two-blade rotor aerodynamic characteristics in hover mode.

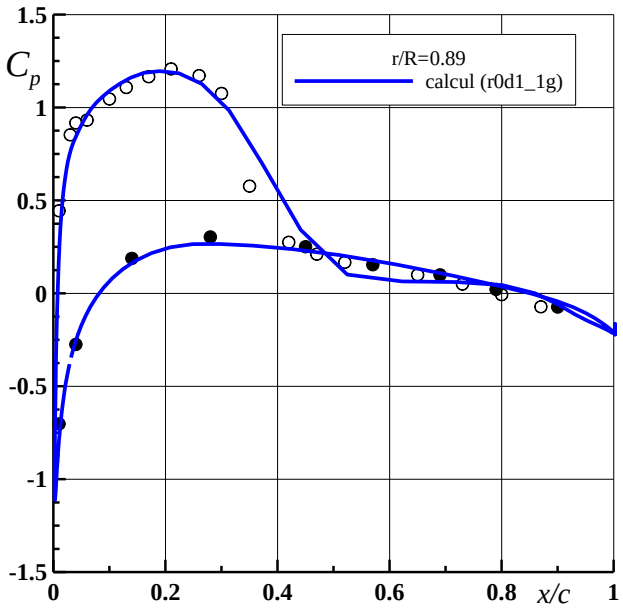

Fig.5. Distribution of pressure coefficient in blade chordwise in r/R=0.89 section. Circles indicate experimental data [3] for upper and lower surfaces. Blue curve shows calculation results

Rotor blades have rectangular plan form and NACA 0012 profile. Geometric twist of blades was missing. Rotor diameter was equal to D=2R=2.286 m, blade chord b=0.1905 m. The chosen computational case (C_T ≈0.0049) corresponded to following experimental conditions at hover: blade angle (collective pitch) α=8° and rotation frequency corresponding to blade tip Mach number M_R = 0.877. The typical Reynolds number calculated by profile chord and tip speed was corresponding to Re=3.93x10^6. The comparison of computational and experimental data is given in Fig.5. It is seen that these data are satisfactorily agreed.

Computational results of flow about rotor in horizontal flight with and without individual blade control are given in Figs.6 and 7. The essential effect in pressure distribution is observed when blades are controlled individually.

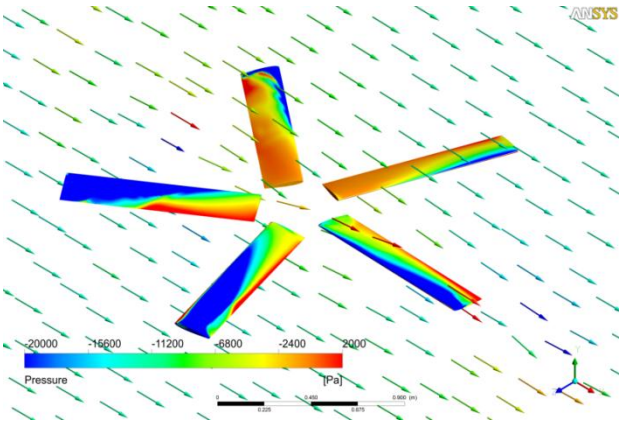

Fig.6. Pressure distribution on blades in forward flight, V/ωR=0.35.

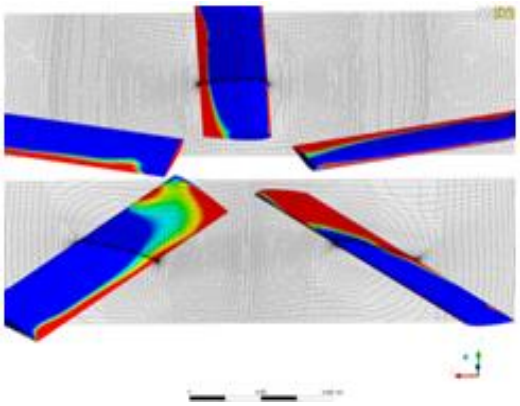

Fig.7. Pressure distribution on blades in forward flight with individual control at blade angle, V/ωR=0.35

4.2.Development and studies of advanced rotor aerodynamic designs

Aerodynamic design of high-speed rotorcraft rotors having triple sweep blade tips for airspeed range of 400-450 km/h was performed in TsAGI. Such rotor models were tested in TsAGI T-104 wind tunnel at flight Mach numbers. The maximum value of figure of merit (FM) in hover reaches the value of 0.75 at high rotor thrust coefficient $C_T/\sigma = 0.23$.

The effect of blade tip turned down (tip of anhedral type) on the figure of merit (relative efficiency) in hover is shown in Fig.8. It is seen that this effect values 0.01-0.015.

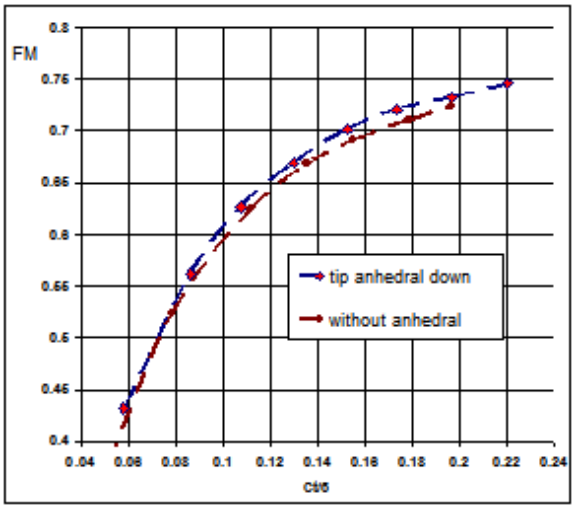

Fig.8. Relative efficiency (figure of merit) in hover

The equivalent lift-to-drag ratio K_{rot} of advanced rotor compared to the current level at the same rotorcraft drag is given in Fig.9. It is seen that the advanced rotor at flight speed of 400 km/h has lift-to-drag ratio equal to the maximum value of modern rotorcraft.

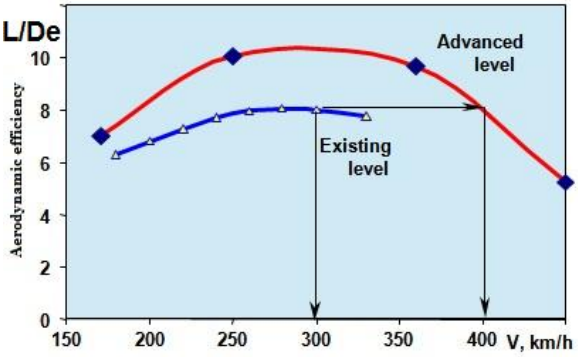

Fig.9. Increasing of main rotor lift-to-drag ratio is clearly observed

A great number of tip types (more than fifteen) were tested in TsAGI for many years. In the course of the tests effective means to influence the blade moment characteristics were found. In particular the rational parameters of leading edge blade shank extensions and the parameters of variable-sweep blade with TsAGI's tip were determined (Fig.10).

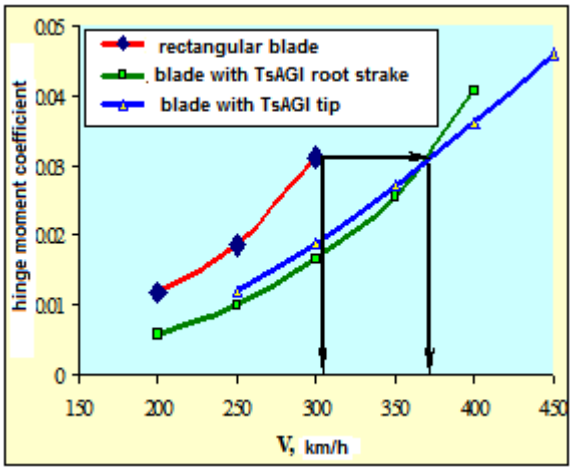

Fig. 10. The effect of rotor blade plan form on hinge moment levels (C_T / σ=0.12, α=-10°, $\omega R = 210 \div 220$ м/с)

As seen from Fig.10 the rationally chosen parameters of the leading edge blade shank extension and the rational parameters of TsAGI's variable-sweep blade tip increase the flight allowable speed by 70 km/h at the given constant hinge moment coefficient.

To decrease the negative effect of blade breakaway for high-speed helicopter the problem of using the rotor binding to hub without hinges becomes urgent. Testing of the rotor models with this binding is resumed in TsAGI (Fig.11).

In this figure the substantial deformation of down-directed (downward) blade at $\psi=180^o$ (in the lower right part of the photo) is clearly observed.

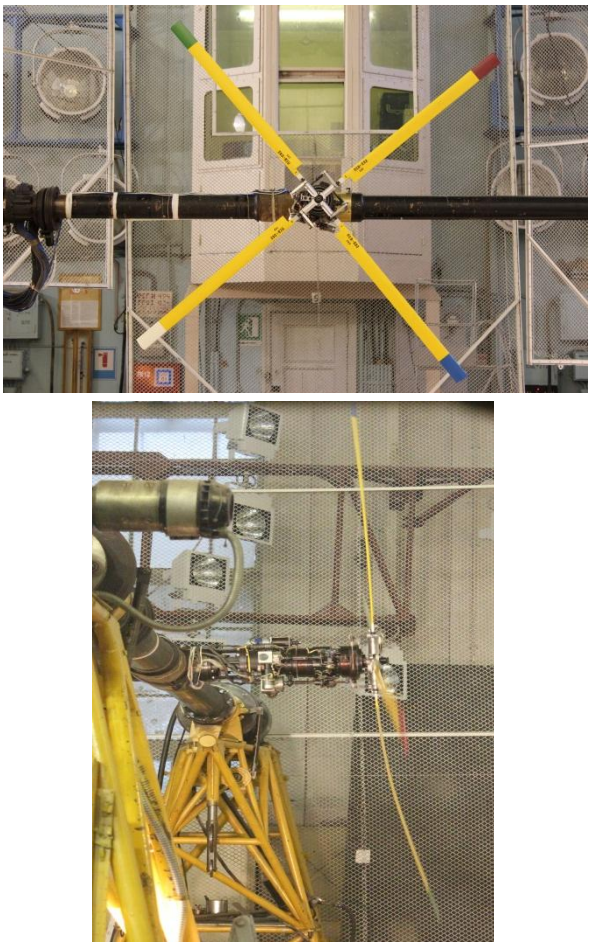

Fig.11. Main rotor model binding to hub without hinges in TsAGI T-105 wind tunnel

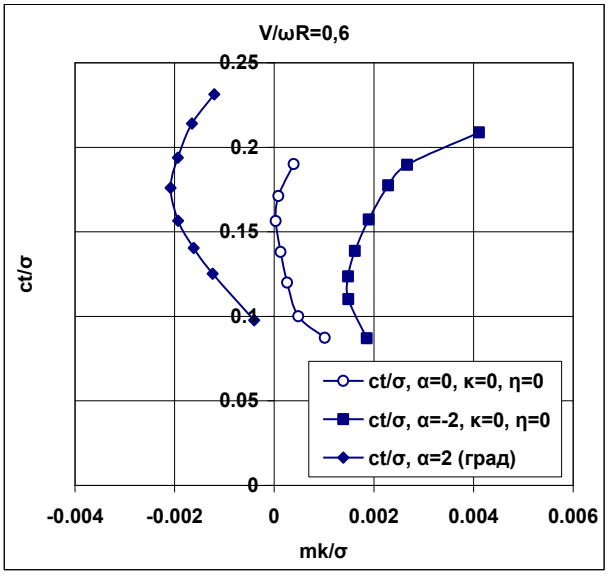

Fig. 12. Main rotor polar at low angels of attack α

In Fig.12 a considerable effect of relatively small variations in rotor angle of attack α = 0, ± 2° on its polar is observed.

4.3.Blade individual control

The calculated estimations of blade individual control effectiveness on vibration acceleration based on computational method [4] are performed. The flow about rotor moving steadily with the average velocity V and rotating relatively to body-axis system with angle velocity Ω is considered. The problem statement is described in [4]. As initial data are taken the blade parameters of Mi-8 helicopter five-blade rotor. Rotor radius R = 8.65 m, chord b = 0.58 m, angle velocity ω = 23.7 rad/s, flight speed V = 100 m/s, blade angle $\varphi_0 = 7.5°$, $C_t/\sigma \approx 0.14$.

It is known that the more the number of rotor blades, the less the pulsation amplitude of rotor thrust coefficient, and hence the vibration acceleration. For five-blade rotor the fundamental transfer harmonic is the fifth one. The rest predominant harmonics (overtones) are multiple to the fundamental harmonic.

The computations show that cyclic fifth-harmonic control of the blade angle has a considerable effect on the blade harmonic thrust amplitude. In Fig. 13 the comparative pattern of vibration acceleration amplitude without control and with combined control by blade harmonic and its two overtones - the 10-th and the 15-th is shown.

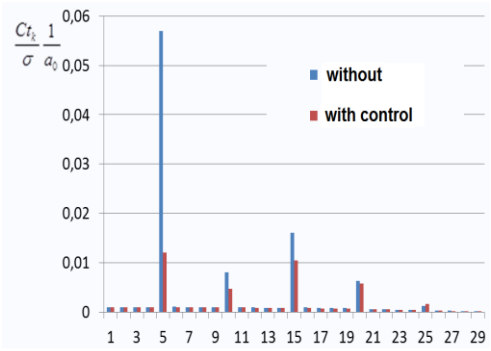

Fig.13. Vibration overload amplitude without control and with combined control by blade harmonic plus its overtones –the 10-th and 15-th (α_o –average load value, k – harmonic number)

It is seen that the blade individual control makes possible to substantially decrease the thrust fluctuations more than 5 times) and overtones (by 2 times). As a result vibration accelerations are transmitted to the body and rotorcraft components also decrease. In this case, as indicated in computations, the average thrust value remains at the same level as without blade individual control.

Thus, studies performed in TsAGI in the last few years show that the blade individual control has a considerable effect on the rotor thrust variables and naturally on the helicopter vibration accelerations.

In recent years experimental investigations are performed in TsAGI in three main directions:

- individual rotor blades control with the help of existing mechanical bench;
- rotor blade airfoil section flow control;
- blade twist and flap control using piezoelectric actuator embedded in the blade.

One of the existing in TsAGI T-105 wind tunnel mechanical benches for individual rotor model blade control is presented in Fig. 14.

Fig.14. Mechanical bench for individual main rotor model blade control

Rotor model characteristics obtained during tests on this bench with blade shank control according to biharmonic law are presented in Fig.15.

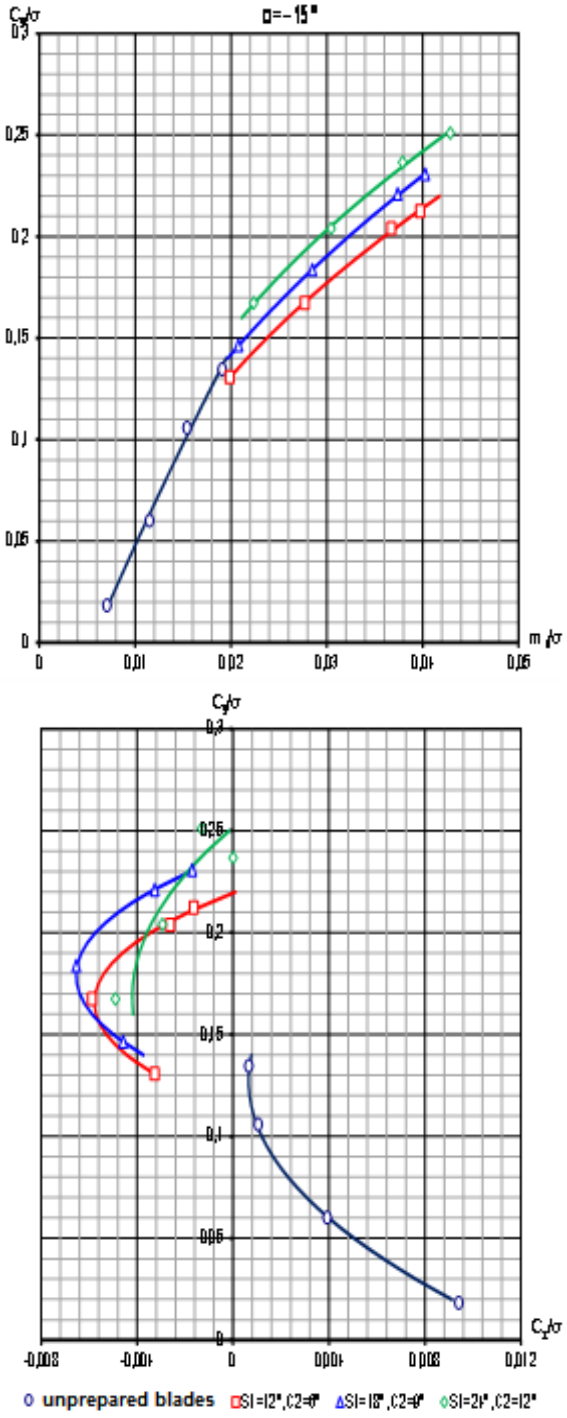

Fig. 15. Blade root sections individual control by biharmonic law, V/ωR = 0.5, s1,c2- sine, cosine Fourier coefficients.

5. ON COMPUTATION OF ROTOR ACOUSTIC CHARACTERISTICS

5.1.Computational results of rotor acoustic characteristics in far field caused by unsteady loads

Time-based realization of sound pressure in different viewpoints in far field at a distance of 150 m from the rotor hub center was determined. For five-blade rotor the dependencies of sound pressure from helicopter azimuthal blade position (in time) in viewpoints corresponding to elevation angle of Θ = 1° and 10° were presented. The calculation was performed by the rotor non-linear theory.

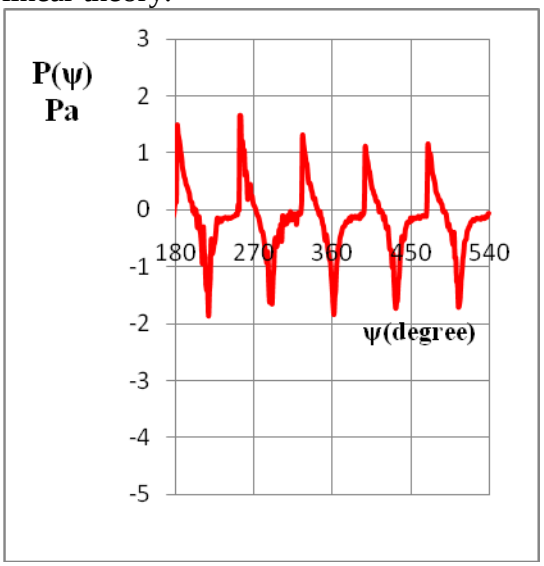

Fig.16. Sound pressure in calculation points vs rotor blade azimuth angle, height angle of Θ = 1°

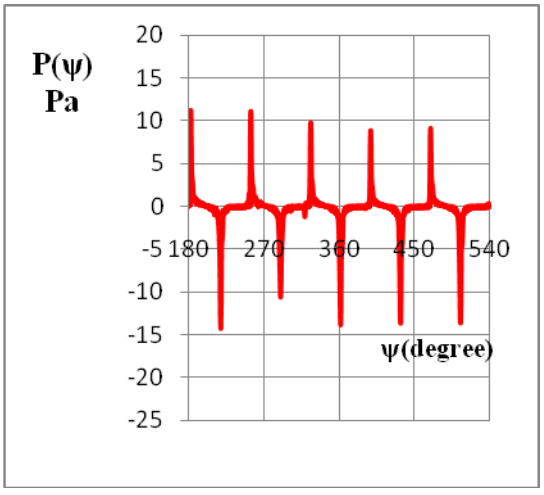

Fig.17. Sound pressure in calculation points vs rotor blade azimuth angle, height angle of Θ = 10°

The behavior feature of indicated time dependencies of sound pressure p(ψ) is that at small elevation angles when the viewpoint is near to the rotor plane of rotation these dependencies differ not only in quantity but also in behavior compared to dependencies p(ψ) for large elevation angles.
Harmonic analysis of dependencies p(ψ) permits amplitude-frequency characteristics to be obtained for the considered calculation example.

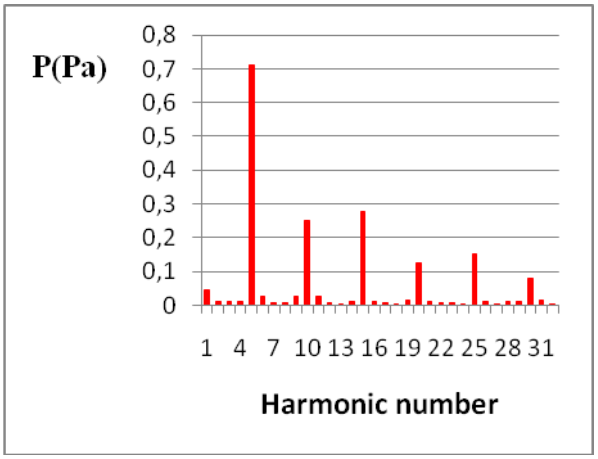

Fig.18. Amplitude-frequency diagram, Θ = 1° above rotor disk plane

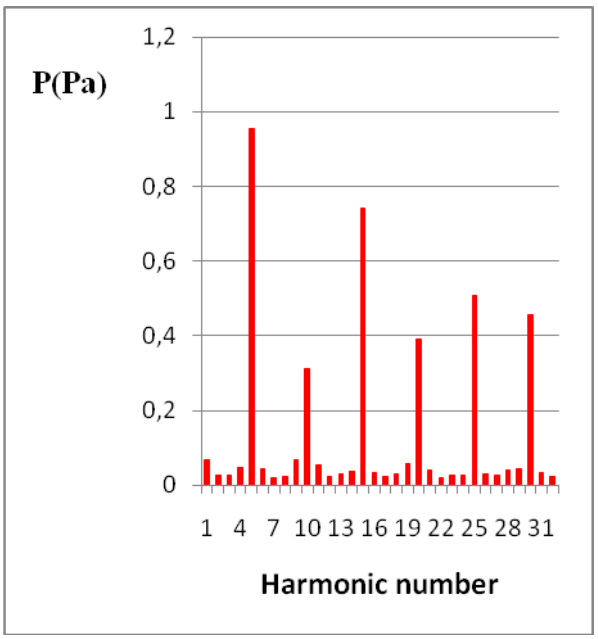

Fig.19. Amplitude-frequency diagram, Θ = 10° above rotor disk plane

In Figs. 18, 19 amplitude-frequency expansion histograms of the rotor sound pressure at viewpoints corresponding to elevation angles Θ = 1° and 10° are presented. It should be noted that the given calculation results of the acoustic characteristics concern the rotor noise caused by the blade unsteady loads including the rotation noise and the load peaks due to periodic behavior of blade flow velocity change and the interaction of blade vortices shedding from the advancing blade tips.

5.2 Computational results of sound pressure caused by the displacement effect associated with blade thickness

Over a period of years the computational method of sound pressure [5-7] in the direction of maximum sound radiation caused by the blade thickness had been developing in TsAGI. Algorithm and computation program of the impulse noise caused by blade thickness were developed. Parametric computation results are presented to estimate the influence of blade tip shape and blade tip velocity on the sound pressure peak level caused by the blade thickness displacement effect. Relationships and influence mechanism (Fig.20) of geometric (tip shape, its sweep angle χ and airfoil thickness ratio $\bar{c}$) and kinematic rotor parameters on the sound pressure peak levels were revealed.

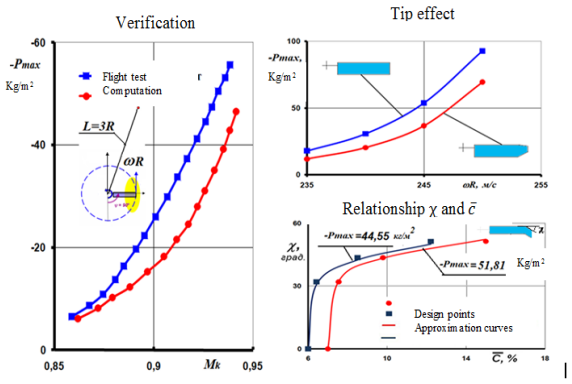

Fig.20. Blade thickness effect on sound pressure

Flight test results published in [8,9] are shown in Fig.20. It is seen in particular that the influence displacement effect in the given test conditions is very considerable. Calculations show that the sound pressure level rises with the increase of thickness ratio at any sweep angle. It is also shown that if the given constant value $-p_{max}$ must be sustained according to the acoustic characteristics then the blade tip can be chosen with the blade thickness, sweep and taper ratio corresponding to this purpose. In this case various combinations of these parameters satisfy the given conditions. Thus, the fulfillment of acoustic requirement opens up the possibility to satisfy other rotor requirements (for example aerodynamic ones) that is to find the optimal solution for one or another problem to ensure the required helicopter performance.

6. AERODYNAMICS OF ROTORCRAFT BODY

Aerodynamics of high-speed helicopter body is extremely important because its drag directly decreases the effectiveness of rotor as propulsive device, increases hinge moments, vibration, etc. As a result additional propulsive system of pusher and tractor propellers type as well as rotary-ring driver and gas-jet system type should be considered. The conventional experimental methods to investigate and work out helicopter body aerodynamics exist in TsAGI. Recently numerical methods based on CFD RANS have been successfully used to study rotorcraft body aerodynamics.
The results of the flow pattern and pressure distribution computation for two helicopter bodies with slip (in the left) and without slip (in the right) are shown in Fig.21.

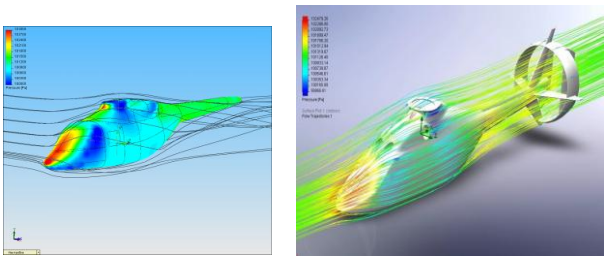

Fig.21. Streamlines and pressure distribution over helicopter bodies

Body calculation aerodynamic characteristics C_D, C_L, C_{M0} are given in Fig.22.

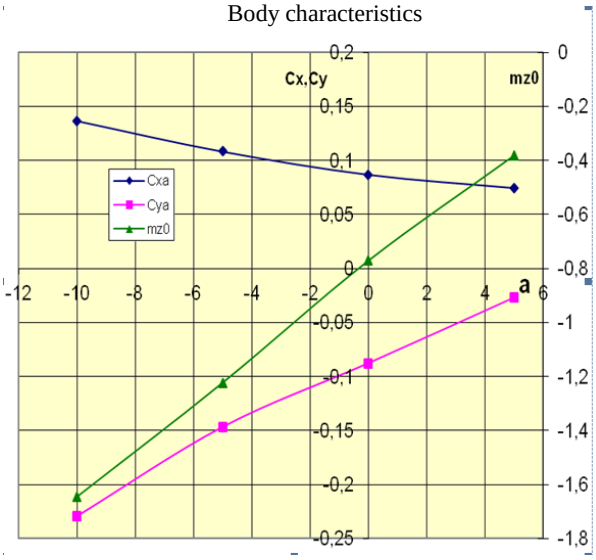

Fig.22. Calculated rotorcraft body aerodynamic characteristics

Example of helicopter body typical tests to study and work out its aerodynamics is shown in Fig.23.

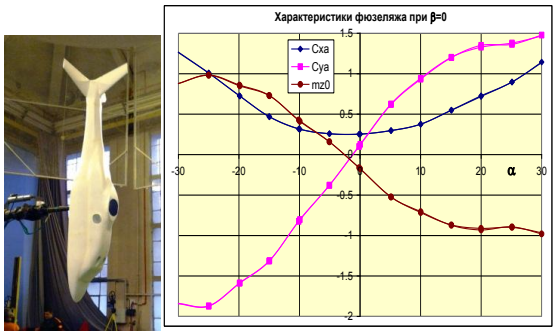

Fig.23. Experimental investigations of helicopter body in TsAGI T-105 wind tunnel

7.THE PROBLEMS OF STRENGTH AND AEROELASTICITY FOR HIGH-SPEED ADVANCED ROTORCRAFT

The loads for high-speed advanced rotorcraft considerably increase, and growth of flight speeds intensifies the problems of protection from aeroelasticity phenomena.

To assure high weight perfection of the rotorcraft construction it is necessary to strive for more detailed simulation at initial development stages.
The use of finite-element simulation with detailed description of the construction components makes possible the more accurate analysis of the structure strength and selection of the most optimal structural and loading pattern.
The example of modern simulation of structure loading pattern is shown in Fig.24.

The parameters of finite-element rotorcraft model are presented in the table.

Type of element	Number of elements
QUAD	212484
TRI	863
NODE	208660
DOFs	~ 1050000

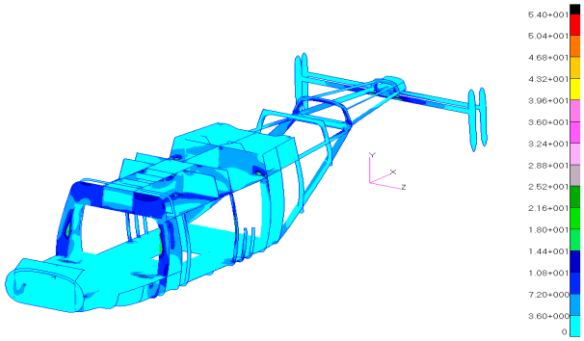

Fig.24

Stress levels in structure components are presented in Fig.24.
It should be noted that the use of composite materials is appropriate for helicopter body structure. Several zones of the body need more detailed investigation as shown in Fig.25.

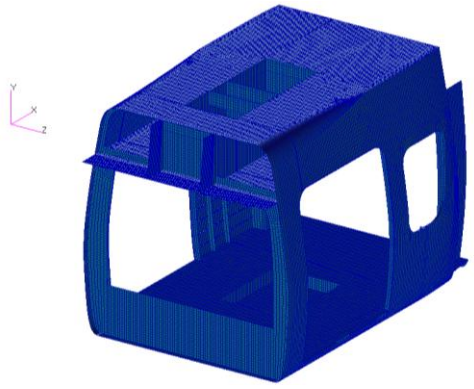

Fig.25

At present the technology has been developed for tail rotor blades production using composite materials as shown in Fig. 26.

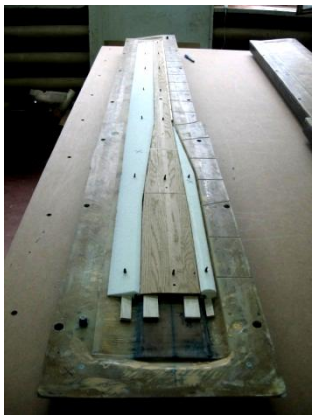

Fig.26

The methods and the means of development of structure service life as well as transmission must be improved because of the vibratory loads growth. Passive and active methods to suppress oscillations are introduced into practice. The test bench base is being developed for body service life work out at multicomponent loading. Methods to investigate rotor and tail rotor flutter of high-speed helicopter with the account of nonlinearity in blade composite structures as well as control system are being developed.

8.DEVELOPMENT OF ROTORCRAFT DIGITAL FLY-BY-WIRE CONTROLS

To advance the future helicopter control systems the possible use of digital fly-by-wire controls is studied. In TsAGI there are two piloted simulators (Fig.27) for semi-full-scale simulation to carry out the appropriate investigations

Fig.27. TsAGI's research full-scale piloted simulator, compact simulator

As an example in Fig.28 is presented the fraction of FLY-BY-WIRE CONTROLS

.

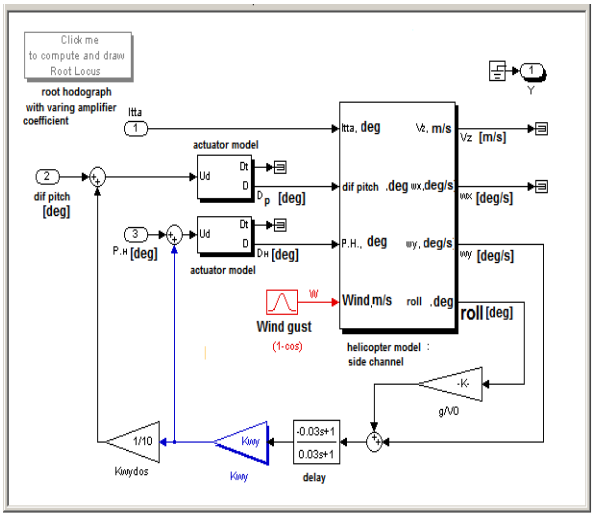

Fig.28. Couple control by rudder and differential varying collective pitch in yaw damper

In the course of tests the following is obtained:

- principal control circuits for two configurations are determined: with coaxial "rigid" rotor and with tandem rotors;
- functional algorithm composition of digital fly-by wire controls is determined;
- digital fly-by-wire controls architecture variants are developed to ensure the required flight level safety;
- requirements to actuators and calculators of fly-by-wire controls are determined;
- algorithms of fly-by-wire controls are developed.
-

9.AIR DATA SYSTEMS

The successful completion of modern helicopter state joint tests is an important outcome in recent years. This rotorcraft has a brand new air data system SIVPV-52 developed in TsAGI and "Aeropribor Voshod" corporation. This all-aspect angle and high-precision system (Fig.29a) ensures air data measurements at any flight regimes including low speeds (up to hover) and flights in arbitrary direction (forward-backward, to the left-to the right, upward-downward). As an example in Fig. 29b is presented the comparison of side airspeed $V_{z\ sivpv}$ measured using SIVPV system and reference speed $V_{z\ ref}$ obtained with the help of JPS. It is seen that variation in measurement does not exceed 5 km/h. It should be noted that previously used standard air data system could not measure the side airspeed in principle.

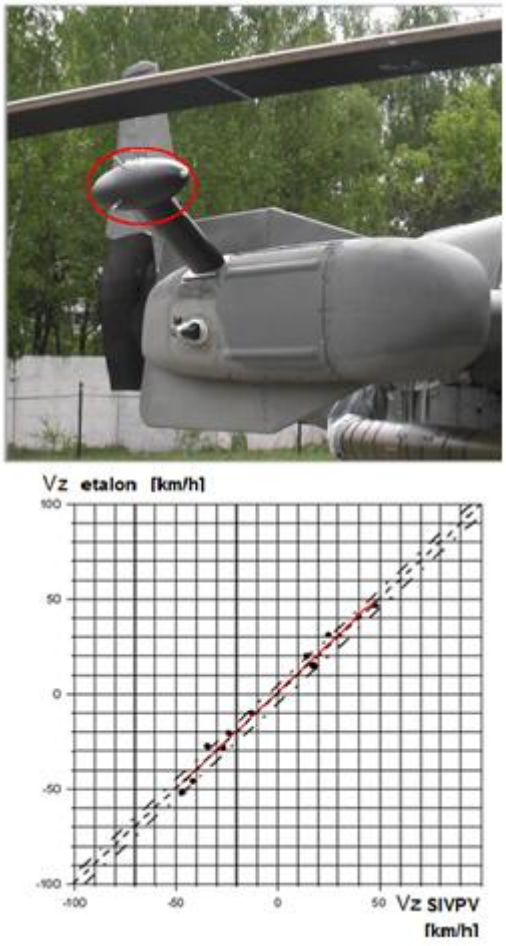

Fig.29. Rotorcraft air data system SIVPV -52. Measurement of side airspeed

CONCLUSION

TsAGI research associated with scientific-technical backlog based on the essential development of work-out technology and high-speed helicopter investigations ensures considerable improvement of aerodynamic, acoustic, strength, aeroelastic, flight maneuverable and economic characteristics. This research enables the Russian helicopter companies to develop innovative competitive state-of-the-art designs.

COPYRIGHT STATEMENT

REFERENCES

1. Golovkin M.A. Development of TsAGI Research on Rotorcraft Aerodynamics during 2008-2009. Proceedings of 9-th Forum RVO, 2010.
2. Commercial version ANSYS CFX Ver. 13.0.
3. Caradonna F.X., Tung C. Experimental and Analytical Studies of a Model Helicopter Rotor in Hover // NASA TM 81232, 1981, P. 60.
4. Kritsky B.S. Mathematical Model of Rotary-wing Aircraft. TsAGI Proceedings, issue 2655, 2002, pp.50-56.
5. Baskin V.E. Acoustic Pressure Caused by Rotorcraft Rotor at Horizontal Flight. TsAGI Proceedings, issue 1373, 1972.
6. Baskin V.E. On Linear Theory of Gas Nonstationary Motion under the Effect of

Nonpotential External Forces. Izvestiya Academii Nauk SSSR. Fluid and Gas Mechanics №4, 1969.
7. Golovkin V.A., Kritsky B.S., Mirgazov R.M. On Calculation of Rotor Displacement Noise Induced by Blade Thickness, Uchenye Zapisky of TsAGI v.XLI, №5, 2010.
8. Aeroacoustic research – an army perspective helicopter. Andrew Morse, Fredric H. Schmitz NASA Conference Publication 2052 Part I, Part II Helicopter Acoustics May 22-24, 1978.
9. Schmitz F.H., Boxwell D.A. In-Flight Far-field Measurement of Helicopter Impulsive Noise, 32nd Annual National Forum AHS Preprint № 1062, 1976.tune